Artificial Neural Network Based Algorithm for Fault Detection in a Ring DC Microgrid Under Diverse Fault Conditions

Shankarshan Prasad Tiwari

Ph.D. Scholar, Department of Electrical Engineering, National Institute of Technology Raipur, Chhattisgarh, India
E-mail: shankarshan.tiwari20@gmail.com

Received 13 June 2022; Accepted 22 July 2022;
Publication 09 December 2022

Abstract

The DC microgrid has become a greater power system in modern power technology due to its wider acceptance as compared to the AC-based traditional power distribution network. Nevertheless, protection of the DC microgrid is a difficult and complicated task due to numerous types of fault scenarios such as pole-to-ground and pole-to-pole faults, variation in fault current magnitude during grid connected and islanded mode, as well as bidirectional behaviour of the converters. In addition to the abovementioned challenges, fault detection during varying fault resistance and intermittency is also a crucial and tricky task because the level of the fault current can vary due to the distinct value of the fault resistance. Therefore, in this manuscript, an ANN-based protection scheme is proposed to detect the fault under varying fault conditions. Furthermore, to investigate the appropriateness of the protection scheme, DT and kNN-based techniques have also been considered for analysis purpose. In the proposed protection scheme, the tasks of mode identification, fault detection/classification, as well as section identification,

Distributed Generation & Alternative Energy Journal, Vol. 38_1, 23–40.
doi: 10.13052/dgaej2156-3306.3812

have been proposed. The results in Section 5 indicate that the protection scheme is capable and accurate for fault detection in any type of faulty condition.

Keywords: DC microgrid, artificial neural network (ANN), fault detection/classification, pole to ground and pole to pole fault, distributed energy resources (DERs).

1 Introduction

In the modern era, the crisis of power is tremendously increasing due to advancements in industrial and commercial infrastructure. To meet the required power demand for the reduction of this type of energy crisis, various types of power generating sites are installed in all over the world, where majority of them are based on coal, nuclear fuel, and some other petroleum products. The common drawbacks with such plants are the emission of hazardous particles into the atmosphere and their dependency on the available fossil fuels. Therefore, the traditional energy scenario is continuously shifting towards the adoption of alternate sources of energy such as solar [1, 2], geothermal, wind, and biomass for the further utilization [3–5] and this has led to the concept of a small-scale microgrid as a future power generation technology. The microgrid is the integration of low-rated distributed energy resources, converters, energy storage devices [6], and loads with some clearly defined electrical boundaries [7, 8]. On the basis of category, microgrids can be classified as AC, DC, or hybrid microgrids [9]. In recent times, utilization of DC-based appliances has been tremendously increasing in various applications such as shipboard power systems, residential loads [10], power system control devices, data centers [11], and lighting appliances [12]. Therefore, the DC microgrid has attained wide acceptance in various fields. The DC microgrid offers numerous benefits over AC-based systems, such as environmental friendliness, efficient and reliable [13], absence of frequency [14], no need for synchronization, safer for human bodies, higher power transfer capability, and fewer conversion stages of power. Nevertheless, the protection of DC microgrids is a challenging task due to various types of challenges, such as variation in the magnitude of fault current during grid connected and islanded mode as well as varying nature of fault resistances, types of fault as PG and PP fault (pole to ground and pole to pole fault), absence of zero crossing, and limited fault current capacity of converters. To illustrate the problems related to the varying fault resistances and their effects on

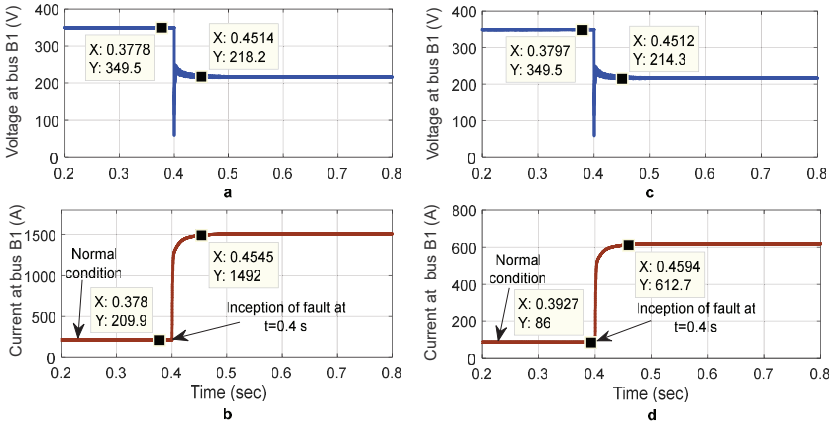

Figure 1 Dissimilarities in voltage and fault current magnitude during grid connected (a), (b), and islanded modes (c), (d).

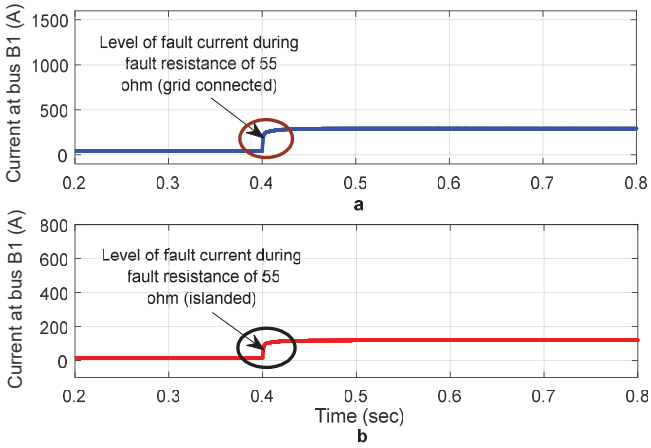

Figure 2 (a) Level of the fault current during high-fault resistance (grid connected mode). (b) Level of the fault current during high-fault resistance (islanded mode).

the fault current, Figures 1 and 2 have been considered. In Figure 1, (a) pole-to-ground fault has been created at t = 0.4 s under grid connected and islanded mode, and the test model has been simulated for a time duration of t = 0.8 s. The results in the proposed figure indicate that the magnitude of the fault is higher due to the low value of fault resistance, while, it is less in (Figure 2) due to greater value of fault resistance. Therefore, detection of the fault is tricky and difficult. Figure 1, (a) and (b) are depicted for grid

connected mode, while (c) and (d) are dedicated for islanded mode. Similarly, Figure 2, (a) is illustrated for grid connected mode and (b) for islanded mode of operation under pole-to-ground fault. A number of literatures have been reported by the authors regarding DC microgrid protection, such as protection scheme for ring based DC microgrid in [15], differential current based fault detection in [16], centralised strategy based DC microgrid protection in [17], high speed differential strategy in [18], and transient analysis based protection scheme [19], Firefly algorithm-based DC microgrid protection scheme in [20], a non-unit protection scheme for DC microgrid [21], a non-iterative protection framework in [22], and poverty severity index-based protection scheme [23]. However, in reported protection schemes, the impact of the varying fault resistance has not been analysed, as well as the protection schemes have also been not analysed under the distinct level of wind speed and solar irradiance. Under such circumstances and difficult operating conditions, the protection scheme must be invulnerable and accurate. Therefore, in this article, an ANN (artificial neural network-based) algorithm is proposed to provide immunity to the system after detection of unhealthy faulty conditions. The major highlights of this article are:

[1] Development of a protection scheme which can easily detect the faults under varying dynamics of the fault parameters.
[2] Validation of protection scheme under different types of faulty conditions.
[3] Analysis of the protection scheme to evaluate the accuracy of the mode detector, fault detector/classifier, and section identifier under grid connected and islanded mode.
[4] Comparison of proposed work with other reported techniques for analysis of the appropriateness of protection scheme.

The rest of the manuscript is organised as follows: Section 2 describes the DC test microgrid model to simulate the fault scenarios, while Section 3 deals with the description of the ANN-based algorithm. In Sections 4 and 5, development of protection scheme and performance evaluation are given, while in Section 6, conclusion of the proposed work is given. In Section 7, references are given.

2 Single Line Diagram of DC Microgrid System

The single line diagram of a 500 kW DC microgrid model with a ring configuration is illustrated in Figure 3. In the proposed DC microgrid system,

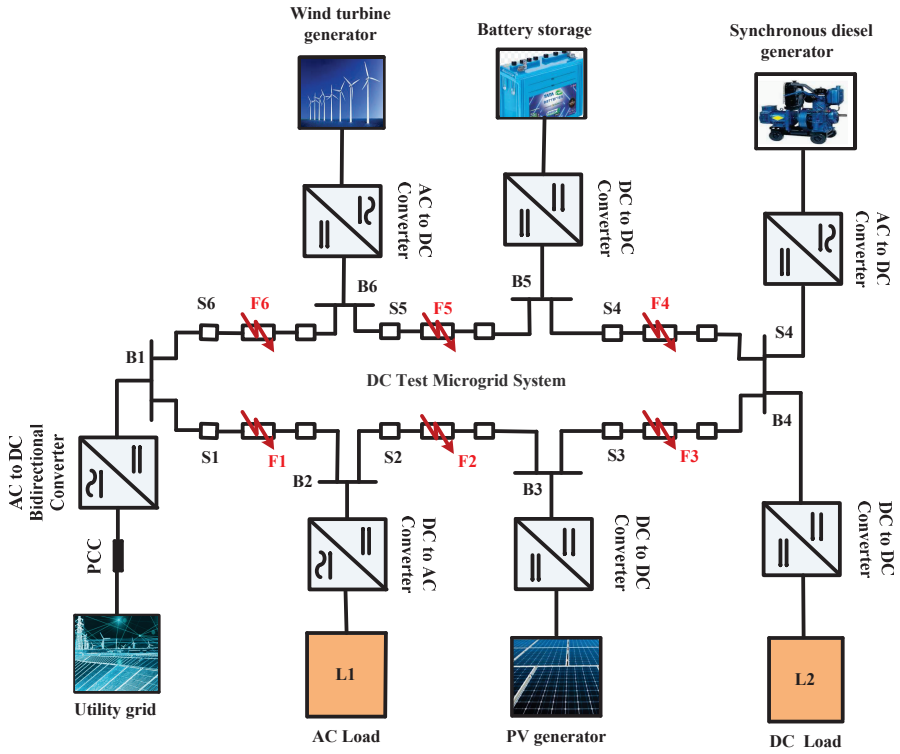

Figure 3 Single line diagram of DC microgrid system.

three DERs (distributed energy resources) such as photovoltaic generators, synchronous diesel generators, and wind turbine generators are integrated at different locations in the system. Further, for energy management purposes, a battery has also been incorporated. The proposed system consists of the six buses in the entire system, namely B1, B2, B3, B3, B4, B5, and B6, respectively, as well as six sections from S1 to S6. As discussed earlier in this section, the DERs are located at different positions, therefore power electronics converters are connected between the sources and ring of the DC microgrod. The entire length of the system is extended over six kilometers, where each section is stretched over a length of one kilometer. Two loads, L1 and L2, are connected by buses B3 and B4 respectively. The utility grid is connected to bus B1 with the help of the bidirectional converter, therefore microgrid can be operated into islanded mode also if the utility grid is disconnected [24] due to fault.

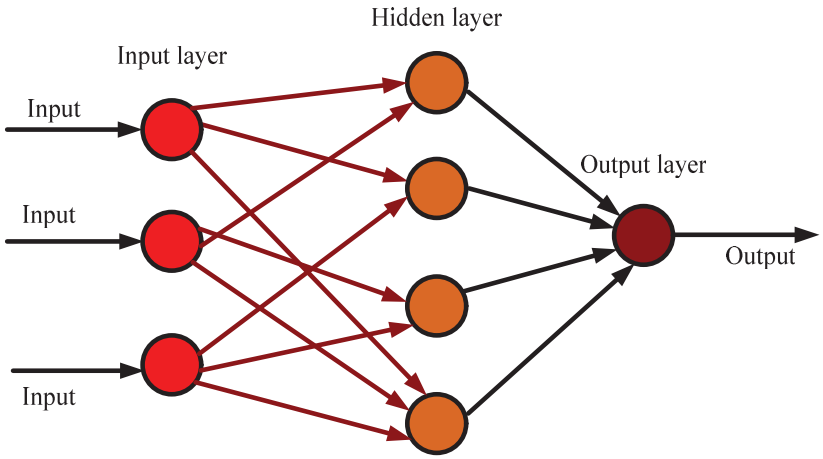

Figure 4 Architecture of artificial neural network.

3 Outline of the Artificial Neural Network (ANN)

In recent times, ANN (artificial neural network) has become an emerging tool for diagnosis of faulty conditions in the power system network [25–27]. To understand the operation of the artificial neural network, Figure 4 is considered where the basic architecture of the ANN is given with details of the network. The proposed algorithm consists of three layers: an input layer, a hidden layer, and an output layer. There are many hidden layers inside the network that connect each layer for appropriate operation of the system. To process the data from input to output layer, various nodes are utilised by the network, which is called artificial neurons. The performance of the artificial neurons can be compared with that of the units of biological neurons in the brain. To train the ANN modules samples of the voltage and current are utilised to design the input and target dataset from bus B1.

4 Flow Chart of the Proposed Algorithm for Fault Detection-Classification and Section Identification

In this section, the flow chart of the ANN-based protection scheme is proposed and illustrated in Figure 5, where the sequence of operations to perform the intended tasks such as mode detection, fault detection, classification, and section identification can be easily observed. In order to identify the mode of operation such as GC (grid-connected) and IM (islanded mode), ANN-1 has

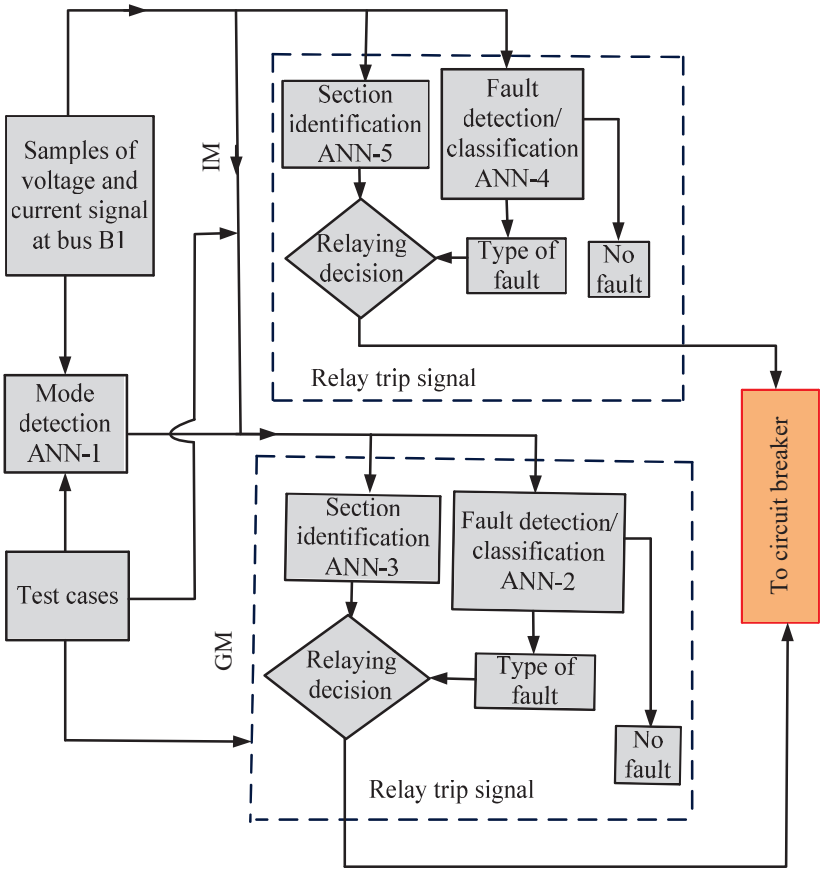

Figure 5 Protection scheme based on artificial neural network (ANN).

been developed with levels of 0 and 1. On the basis of the output of the mode detector module, the remaining modules of the algorithm will be automatically active. Therefore, for tasks of fault detection/classification, and section identification in each mode, a total of four ANN modules have been developed, as illustrated in Figure 5. In grid connected mode, ANN-2 and ANN-3 are utilized, where ANN-2 is considered for fault detection/classification, while ANN-3 is for section identification. Similarly, ANN-4 and ANN-5 are considered during islanded mode for the same task. Once the fault type and faulty section are identified, the relay will issue a trip signal to operate the circuit breaker. To test all the ANN modules in the proposed algorithm, a number of test cases have been considered under dissimilar fault parameters.

5 Performance Analysis

The high performance of any protection scheme decides the invulnerability and reliability of the system. Therefore, in this section, the performance of the protection scheme has been examined for mode detection, fault detection/classification, and section identification of the proposed system. A total of 7056 fault cases have been generated under both of the modes, including 500 no fault cases from different conditions such as variation in linear and non-linear load, solar irradiance and wind speed. Various types of fault parameters such as variation in length, fault resistance and fault inception has been considered for generation of datasets. Apart from the above fault parameters, variations in the solar irradiance and wind speed have also been considered as earlier described. To observe the efficacy of the protection scheme, a number of test cases have been considered for training and testing of the modules. A total of six subsections have been considered for analysis of the ANN modules.

5.1 Mode Detection Module (ANN-1)

To analyse the appropriateness of the mode detection module (ANN-1), a total number of 1967 test cases have been considered, then the percentage accuracy has been analyzed to investigate the accuracy of the mode detector module. After successful testing of the proposed mode detector, it has been found that the accuracy of the mode detector is 100% during the grid-connected as well as islanded mode of operation.

5.2 Fault Detectiopn/Classification Modules (ANN-2 and ANN-4)

The accurate fault detection for any protection scheme is an important task to ensure the reliability of the system. Hence, like the mode detection module, ANN-2 AND ANN-4 modules have also been tested. A total of 1862 test cases have been considered during the grid connected and islanded mode of operation, with 150 no-fault cases. The overall accuracy under both modes is illustrated in Table 1. Two reliability indices, dependability and security, have been considered for investigation of the protection scheme, where dependability ensures the actual detection of fault cases out of total given fault cases, while security ensures the generation of the false alarm signal. If the accuracy of the security is high, then the probability of the false generation of the alarm signal is lower, while higher accuracy of dependability can increase the accurateness of the protection scheme for fault detection. Further, to

Table 1 Performance of the fault detector/classifier in terms of dependability and security

	Type of Mode					
	Grid Connected			Islanded		
Name of Algorithms	Dependability (%)	Security (%)	Overall Accuracy (%)	Dependability (%)	Security (%)	Overall Accuracy (%)
ANN	98.97	100	**99.48**	98.11	100	**99.05**
DT	97.63	98.88	**98.25**	96.33	97.33	**96.83**
Standalone kNN	96.55	97.63	**97.09**	95.77	96.76	**96.26**

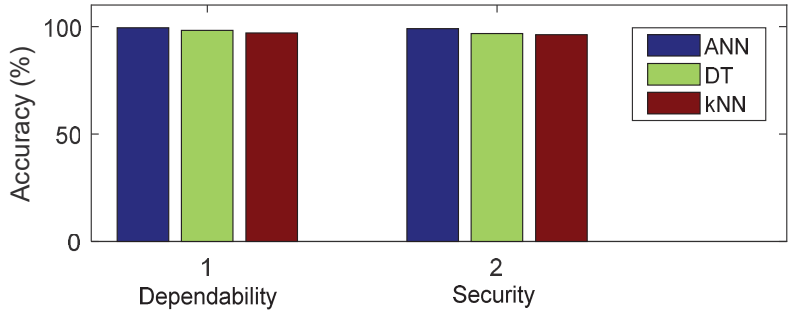

Figure 6 Comparison of detected accuracy in grid connected mode.

examine the performance of the proposed fault detector/classifier, two other techniques, i.e., DT and kNN, have also been considered and tested for the same datasets. The accuracy of the proposed fault detector classifier reveals that the scheme outperforms and is immune in cases of adverse conditions in the power distribution network. Further, to depict the differences in the accuracy during fault detection a bar graph is plotted in Figure 6 where variation in the percentage accuracy can be easily analysed.

5.3 Section Identification Module (ANN-3 and ANN-5)

To ensure the appropriate continuity of power supply without any long interruption in the consumer side, it is a must to identify the faulty section quickly in the existing power distribution network. Rapid identification of faulty section helps in the reduction of the serious hindrance in the system by earlier restoration of the power supply. Therefore, in this subsection, the performance of the section identifier is examined. ANN-3 and ANN-5 are used for identification of the faulty section in both modes of operation.

Table 2 Performance of ANN-3 and ANN-5 for section identification

Mode of Operation	Section	No of Test Cases	ANN (Accuracy %)
Grid connected mode	S1	160	98.71
	S2	158	98.73
	S3	139	98.63
	S4	158	98.41
	S5	160	98.75
	S6	156	97.89
	Overall accuracy %		**98.52**
Islanded mode	S1	158	97.95
	S2	156	97.22
	S3	160	97.88
	S4	139	97.44
	S5	160	97.27
	S6	158	97.39
	Overall accuracy %		**97.52**

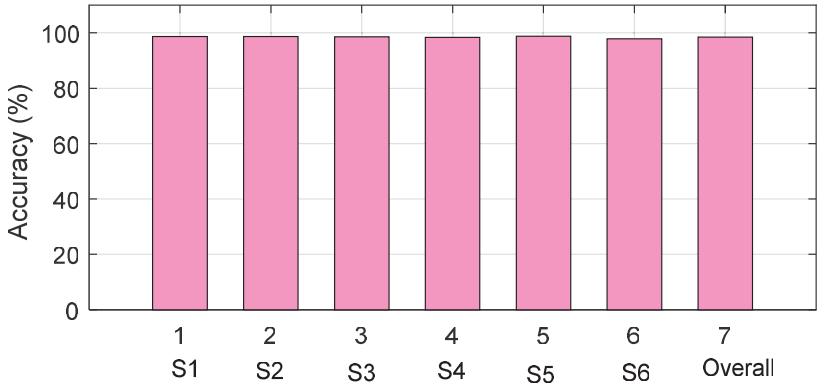

Figure 7 Comparison of percentage accuracy during section identification (grid-connected).

To perform the section identification task, a total of 1862 test cases were considered in grid connected and islanded mode, and the performance is summarised in Table 2. All sections from S1 to S6 have been taken into account for investigation of the faulty sections in entire DC microgrid. The accuracy during the section identification (pole to ground fault) is 98.52% and 97.52%, respectively, for grid connected and islanded mode. Further, to demonstrate the detection accuracy of faulty sections by proposed section identifiers, two plots (bar plots) are depicted in Figures 7 and 8, where differences in the percentage accuracy can be easily observed.

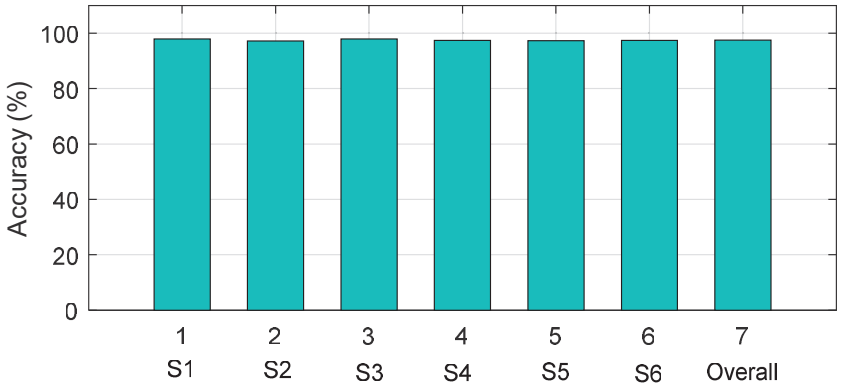

Figure 8 Comparison of percentage accuracy during section identification (islanded-mode).

5.4 Response of the Protection Scheme Against PG, PP Fault and Distinct Fault Resistance Under Grid Connected and Islanded Mode

In this subsection, the immunity of the protection scheme has been evaluated, and the response of the protection scheme under stressed conditions is dealt with in the below table. The range of the fault resistance is considered between 5 to 100 ohm for both of the modes. For pole to pole fault, value of the fault resistance is 0.1 ohm instead of higher value because it is too much smaller when compared with pole to ground fault (in pole to ground fault conditions can vary due to contact of the conductor with dissimilar surfaces such as sand, branches of trees, wet surfaces while constant for pole to pole fault). The wind speed is considered between 3 to 15 m/s while solar irradiances between 100 to 1000 W/m^2. Results in Tables 3 and 4 indicate that the protection scheme outperforms during stressed conditions and accurately responds for each section when a pole to ground and pole to pole fault has been created. The generation of the trip signal under pole to ground is depicted in Figures 9 and 10, where it can be seen that the protection scheme is capable to detect the fault rapidly.

5.5 Robustness of the Protection Scheme Under Different Fault Inception and Type of Fault

The accuracy of the protection scheme under different fault inceptions has been evaluated in this subsection. Further responses of the ANN modules are demonstrated in Table 5. Pole to ground as well as pole to pole faults

Table 3 Response of the protection scheme for pole to ground fault under distinct solar irradiance and wind speed

Types of Mode	Type of Fault	Fault Resistance (Ω)	Solar Irradiance (W/m^2) and Wind Speed (m/s)	Faulty Section	Response of ANN	Relay Response Time (m/s)
Grid connected	PG	10	100 W/m^2, 5 m/s	S1	PG	1.7
	PG	15	200 W/m^2, 8 m/s	S4	PG	1.5
	PG	25	400 W/m^2, 10 m/s	S3	PG	1.5
	PG	40	600 W/m^2, 13 m/s	S6	PG	1.8
	PG	50	700 W/m^2, 15 m/s	S5	PG	1.7
	PG	55	1000 W/m^2, 6 m/s	S1	PG	1.6
	PG	75	800 W/m^2, 9 m/s	S2	PG	1.8
	PG	100	300W/m^2, 10 m/s	S5	PG	1.6
Islanded mode	PG	20	200 W/m^2, 3 m/s	S4	PG	1.8
	PG	35	300 W/m^2, 10 m/s	S1	PG	1.7
	PG	40	500 W/m^2, 14 m/s	S3	PG	1.7
	PG	45	400 W/m^2, 12 m/s	S1	PG	1.9
	PG	65	500 W/m^2, 8 m/s	S6	PG	1.7
	PG	85	800 W/m^2, 7 m/s	S5	PG	1.8
	PG	90	700 W/m^2, 5 m/s	S3	PG	1.7
	PG	100	800 W/m^2, 10 m/s	S2	PG	1.8

Table 4 Response of the protection scheme for pole to pole fault under distinct solar irradiance and wind speed

Types of Mode	Type of Fault	Fault Resistance (Ω)	Solar Irradiance (W/m^2) and Wind Speed (m/s)	Faulty Section	Response of ANN	Relay Response Time (m/s)
Grid connected	PP	0.1	100 W/m^2, 5 m/s	S1	PP	1.5
	PP	0.1	200 W/m^2, 8 m/s	S4	PP	1.4
	PP	0.1	400 W/m^2, 10 m/s	S3	PP	1.4
	PP	0.1	600 W/m^2, 13 m/s	S6	PP	1.7
	PP	0.1	700 W/m^2, 15 m/s	S5	PP	1.6
	PP	0.1	1000 W/m^2, 6 m/s	S1	PP	1.6
	PP	0.1	800 W/m^2, 9 m/s	S2	PP	1.5
	PP	0.1	300W/m^2, 10 m/s	S5	PP	1.5
Islanded mode	PP	0.1	200 W/m^2, 3 m/s	S4	PP	1.6
	PP	0.1	300 W/m^2, 10 m/s	S1	PP	1.5
	PP	0.1	500 W/m^2, 14 m/s	S3	PP	1.6
	PP	0.1	400 W/m^2, 12 m/s	S1	PP	1.8
	PP	0.1	500 W/m^2, 8 m/s	S6	PP	1.7
	PP	0.1	800 W/m^2, 7 m/s	S5	PP	1.8
	PP	0.1	700 W/m^2, 5 m/s	S3	PP	1.6
	PP	0.1	800 W/m^2, 10 m/s	S2	PP	1.7

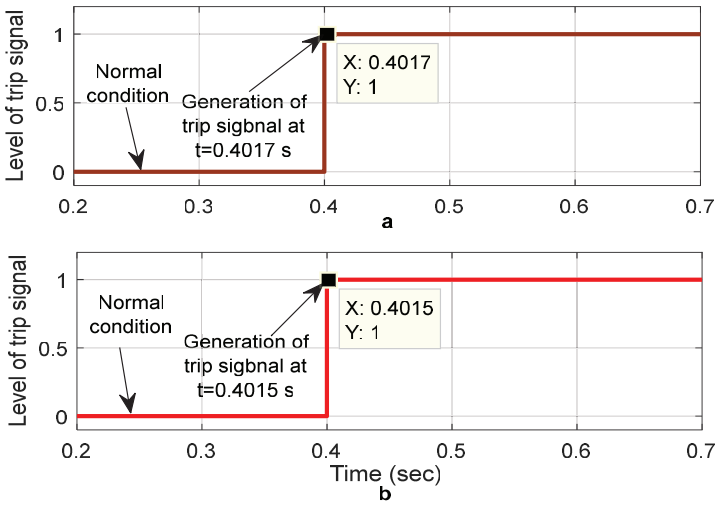

Figure 9 Trip signal generation for PG fault (grid-connected).

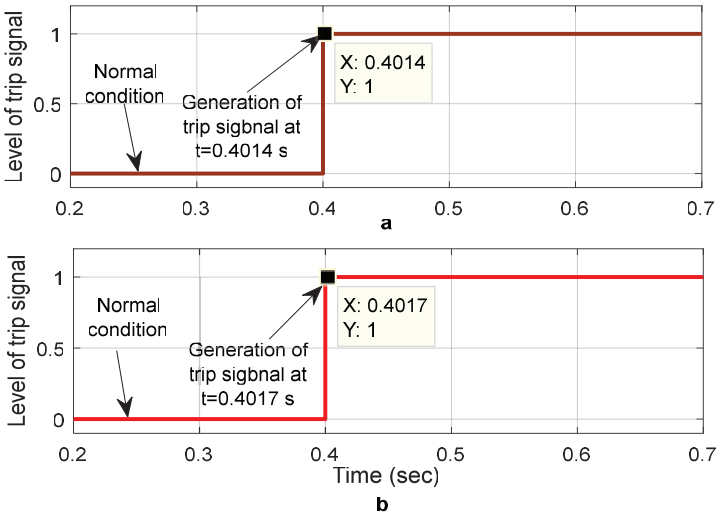

Figure 10 Trip signal generation for PP fault (grid-connected).

have been considered for analysis of the protection scheme under dissimilar fault conditions. In case of PG fault, fault resistance can vary due to different grounding conditions, so the magnitude of the fault current can vary from low to high value (for PP fault low value of fault resistance has been considered for analysis purpose). The result in the below table indicates the immunity

Table 5 Response of the protection scheme under distinct fault inception and low and high fault resistance

Types of Mode	Type of Fault	Fault Resistance	Faulty Inception	Response of ANN
Grid connected	PG	20	0.4	PG
	PG	45	0.6	PG
	PG	60	0.8	PG
	PG	70	0.5	PG
	PP	0.1	0.2	PG
	PP	0.1	0.4	PG
	PP	0.1	0.3	PG
	PP	0.1	0.1	PG
Islanded mode	PG	55	0.4	PG
	PG	65	0.6	PG
	PG	75	0.8	PG
	PG	85	0.5	PG
	PP	0.1	0.2	PG
	PP	0.1	0.4	PG
	PP	0.1	0.3	PG
	PP	0.1	0.1	PG

Table 6 Performance comparison of the ANN based algorithm with other reported literatures

Parameters of Comparison	[13]	[18]	[15]	Proposed Algorithm
Input features	Voltage and current	Current only	Current only	Voltage and current
Task performed	Detection of fault	Detection of fault	Detection of fault	Mode detection, Fault detection/classification and section identification
Test cases	Not-considered	Not-considered	Not-considered	2167
Stochastic conditions	Not-considered	Not-considered	Not-considered	considered

of the protection scheme is excellent under varying fault resistance and dissimilar fault inceptions.

5.6 Comparison of Proposed Algorithm with Reported Literatures

The performance of the ANN-based algorithm has been analysed in this subsection with some other reported literature as mentioned in the reference.

The parameters during comparison of the protection scheme are illustrated in Table 6. When compared to other reported algorithms, it is concluded that the ANN-based algorithm is reliable and outperforms in terms of all parameters.

6 Conclusion

The DC microgrid offers many advantages over the traditional AC based power distribution network. Nevertheless, the protection of the microgrid is an important task due to the various types of protection issues. In the proposed work for the development of the protection scheme, samples of the voltage and current were utilized in each ANN module. To examine the authenticity of the protection scheme, performance of the protection scheme has been compared with DT and kNN based algorithms for the same datasets. A total of 7056 fault cases were generated through simulation of the proposed DC microgrid model. Results in section 5 indicate that the protection scheme is robust and accurate for detection of the fault under diverse fault conditions.

References

[1] V. Veerasamy, N.I.A. Wahab, M.L. Othman, S.K. Padmanaban, K. Sekar, R. Ramachandran, H. Hizam, A. Vinayagam, M.Z. Islam. LSTM recurrent neural network classifier for high impedance fault detection in solar PV integrated power system. IEEE Access, 2021, 9:32672–32687.

[2] A. Bayu, D. Atinkut, B. Khan. Grid integration of hybrid energy system for distribution network. Distributed Generation & Alternative Energy Journal, 2021,37(3):667–675. https://doi.org/10.13052/dgaej2156-3306.3738

[3] T. Adefarati, R.C. Bansal. Integration of renewable distributed generators into the distribution system: a review. IET Renewable Power Generation, 2009, 10(7):873–884.

[4] S.P. Tiwari, E. Koley, S. Ghosh. Communication-less ensemble classifier-based protection scheme for DC microgrid with adaptiveness to network reconfiguration and weather intermittency. Sustainable Energy, Grids and Networks, 2021, 26, 100460.

[5] S.P. Tiwari, E. Koley, M. Manohar, S. Ghosh, D.K. Mohanta, R.C. Bansal. Enhancing robustness of DC microgrid protection during weather intermittency and source outage for improved resilience and system integrity. International Transactions on Electrical Energy Systems, 2021, 31(12), e13243.

[6] S. Kumar, R.K. Saket, S.K. Padmanaban, J.B. Holm-Nielsen. A comprehensive review on energy management in micro-grid system. Microgrid Technologies, 2021, 1–24.
[7] A. Sharma, S.N. Singh, S.C. Srivastava. Optimal selection of DC microgrid architecture. IEEE 8th Power India International Conference (PIICON),2018, pp. 1–5.
[8] A. Pouryekta, V. K. Ramachandaramurthy. A Hybrid Islanding Detection Method For Distribution Systems. Distributed Generation & Alternative Energy Journal, 2018, 33(4):44–67. https://doi.org/10.13052/dgaej2156-3306.3343.
[9] S.K. Sahoo, A.K. Sinha, N.K. Kishore. Control techniques in AC, DC, and hybrid AC–DC microgrid: a review. IEEE Journal of Emerging and Selected Topics in Power Electronics, 2017, 6(2): 738–759.
[10] D. Salomonsson, L. Soder, A. Sannino. Protection of low-voltage DC microgrids. IEEE Transactions on power delivery, 2009, 24(3): 1045–1053.
[11] R.M. Cuzner, G. Venkataramanan. The status of DC micro-grid protection. 2008 IEEE Industry Appli Society Annua Meet, 1–8.
[12] D Salomonsson, A. Sannino. Load modelling for steady-state and transient analysis of low-voltage DC systems. IET Electric Power Applications, 2007, 1(5): 690–696.
[13] S.J. Iqbal, S.S.Mohammad. Power management, control and optimization of photovoltaic/battery/fuel cell/stored hydrogen-based microgrid for critical hospital loads. Distributed Generation & Alternative Energy Journal, 2022, 37(4):1027–1054. https://doi.org/10.13052/dgaej2156-3306.3747.
[14] S. Dahale, A. Das, N.M. Pindoriya, S. Rajendran. An overview of DC-DC converter topologies and controls in DC microgrid. International Conference on Power Systems (ICPS), 2017; 410–415.
[15] R. Mohanty, A.K. Pradhan. Protection of smart DC microgrid with ring configuration using parameter estimation approach. IEEE Transactions on Smart Grid, 2017, 9(6): 6328–6337.
[16] Dhar S, Dash PK. Differential current-based fault protection with adaptive threshold for multiple PV-based DC microgrid. IET Renewable Power Generation, 2017, 11(6): 778–790.
[17] M. Monadi, C. Gavriluta, A. Luna, J.I. Candela, P. Rodriguez. Centralized protection strategy for medium voltage DC microgrids. IEEE Transactions on power delivery, 2016, 32(1): 430–440.

[18] S.D. Fletcher, P.J. Norman, K. Fong, S.J. Galloway, G.M. Burt. High-speed differential protection for smart DC distribution systems. IEEE Trans on Smart Grid, 2014, 5(5): 2610–2617.

[19] T.R.D. Oliveira, R. Thiago. A.S. Bolzon, P.F.D. Garcia. Grounding and safety considerations for residential DC microgrids, Annual Conference of the IEEE Industrial Electronics Society, 2014, pp. 5526–5532.

[20] S.A. Amamra, H. Ahmed, R.A. El-Sehiem. Firefly algorithm optimized robust protection scheme for DC microgrid. Electric Power Components and Systems, 2017, 45(10): 1141–1151.

[21] A. Meghwani, S.C. Srivastava, S. Chakrabarti. A non-unit protection scheme for DC microgrid based on local measurements. IEEE Transactions on Power Delivery, 2016, 32(1): 172–181.

[22] R. Mohanty, U.S.M. Balaji, A. K. Pradhan. An accurate noniterative fault-location technique for low-voltage DC microgrid. IEEE Transactions on Power Delivery, 2015, 32(1):475–481.

[23] M. Salehi, S.A. Taher, I. Sadeghkhani, M. Shahidehpour . A poverty severity index-based protection strategy for ring-bus low-voltage DC microgrids. IEEE Transactions on Smart Grid, 2019, 10(6), 6860–6869.

[24] O.P. Mahela, Y. Sharma, S. Ali, B. Khan, S.K. Padmanaban. Estimation of islanding events in utility distribution grid with renewable energy using current variations and stockwell transform. IEEE Access, 2021, 9, 69798–69813.

[25] H.R. Baghaee, M. Mirsalim, G.B. Gharehpetian, H.A. Talebi. OC/OL protection of droop-controlled and directly voltage-controlled microgrids using TMF/ANN-based fault detection and discrimination. IEEE Journal of Emerging and Selected Topics in Power Electronics, 2019, 9(3), 3254–3265.

[26] A. Elnozahy, K. Sayed, M. Bahyeldin. Artificial neural network based fault classification and location for transmission lines. IEEE Conference on power electronics and renewable energy (CPERE), 2019, 140–144.

[27] M. Hussain, M. Dhimish, S. Titarenko, P. Mather. Artificial neural network based photovoltaic fault detection algorithm integrating two bi-directional input parameters. Renewable Energy, 2020, 155:1272–1292.

Biography

Shankarshan Prasad Tiwari received the bachelor's degree in Electrical and Electronics Engineering from Rajiv Gandhi Proudyogiki Vishwavidyalaya in 2010, the master's degree in Power System from Rajiv Gandhi Proudyogiki Vishwavidyalaya in 2014, and the Master of Business Administration in Operations Management from Sikkim Manipal University in 2017, respectively. He is currently working as a Ph. D. scholar at the Department of Electrical Engineering, National Institute of Technology Raipur, Chhattisgarh, India. His research areas include power system protection, and artificial intelligence.